

Hyeon-Shik Hwang, ¹ Ph.D.; Kyul Kim, ² B.A.; Da-Nal Moon, ³ D.D.S.; Jae-Hyung Kim, ⁴ Ph.D.; Caroline Wilkinson, ⁵ Ph.D.

Reproducibility of Facial Soft Tissue Thicknesses for Craniofacial Reconstruction using Cone-Beam CT Images

¹ Department of Orthodontics, 2nd Stage of Brain Korea 21, School of Dentistry, Dental Science Research Institute, Chonnam National University, Gwangju, Korea

² School of Dentistry, Chonnam National University, Gwangju, Korea

³ Department of Orthodontics, School of Dentistry, Chonnam National University, Gwangju, Korea

⁴ Department of Oral Medicine, School of Dentistry, Chonnam National University, Gwangju, Korea

⁵ Centre for Anatomy and Human Identification, College of Life Sciences, University of Dundee, Dundee, United Kingdom

Additional information and reprint requests:

Caroline M. Wilkinson, Ph.D.

Centre for Anatomy and Human Identification

College of Life Sciences

University of Dundee

Dow Street

Dundee DD1 5EH, United Kingdom

E-mail: c.m.wilkinson@dundee.ac.uk

Abstract

The purpose of this study was to evaluate the reproducibility of the ST thickness at 31 landmarks using the CBCT images obtained from 20 adult subjects. Four observers carried out ST thickness measurements using Skull Measure (CyberMed, Seoul, Korea) software and the inter and intra-observer reproducibility was evaluated. Only 5 out of 31 landmarks showed significant differences in recorded ST thickness between the observers. When excluding inexperienced observers, all landmarks except for one showed no significant differences between the observers. Regarding the intra-observer reproducibility, the ST thickness measurements at three landmarks showed low correlation coefficients. The results of the present study indicate that CBCT images can be used to measure the ST thickness with high reproducibility. However some landmarks need to be redefined in order to reliably measure ST thickness on CBCT images.

Key words: forensic science, soft tissue thickness, cone-beam CT, craniofacial reconstruction, Korean, reproducibility

Craniofacial reconstruction is a forensic technique which attempts to recreate an individual's face from a skull for the purpose of identification (1,2). Most facial reconstruction techniques employ sets of average values of the facial soft tissue (ST) thickness at some landmark sites (3).

In the past, the reference data of the facial ST thickness were obtained from needle puncturing on cadavers (2). However, these cadaver studies have been criticized due to some inevitable differences between cadaver-based and in-vivo measurements relating to post-mortem tissue changes such as dehydration and shrinkage. In addition, large-scale ST thickness studies using cadavers are limited by subject availability (3). Recently, ultrasound has been utilized for large-scale studies of ST thickness measurements (4-7) and as a non-invasive technique ultrasound systems have several advantages including low cost and accessibility. In addition, it allows measurements in an upright position, unlike cadaver-based measurements that show gravity-related effects due to a supine position. Currently, most craniofacial reconstructions are based on the ST thickness data from ultrasound systems.

While ultrasound systems are simple to use for a large number of subjects, one drawback is that the measurements cannot be repeated and confirmed. Additional landmarks can not be incorporated at a later date. To overcome these disadvantages, computed tomography (CT) has been used to measure the ST thickness. Phillips and Smuts (8) used a dataset of ST thicknesses determined from multi-slice CT scans in a mixed race population. However, the high radiation dose and gravity-related effects inhibited their widespread use because the images are obtained with the subject in a supine position.

Recently-developed cone-beam CT (CBCT) scanner enables images to be obtained with the subject in an upright position. In addition, it was reported that the radiation dose is much lower than from multi-slice CT (9-11). The CBCT images can therefore be used to obtain facial ST thickness measurements for the purpose of a craniofacial reconstruction. The

purpose of this study was to evaluate the reproducibility of ST thickness measurements using CBCT images.

MATERIALS AND METHODS

The CBCT images of 20 adult individuals without facial deformities were selected randomly from the departmental database which were collected from university students in Gwangju, Korea. This research was approved by the Institutional Review Board for the Medical Science at the Chonnam National University Hospital, Gwangju, Korea. Informed consent was obtained from all subjects. The mean age of the subjects was 28.1 years (range 20.1 – 33.6 years). The CT scans were obtained using a CBCT scanner (Alphard Vega, Asahi Roentgen Co., Kyoto, Japan) with a voxel size of 0.39 mm and a FOV of 200 X 179 mm. The subject was scanned in the seated position with a neutral, relaxed, facial expression.

The maxillofacial 3D images were created from DICOM data, which was acquired from the CBCT scans and by using V Works 4.0 (CyberMed, Seoul, Korea). A couple of 3D object files were created with an adjustment of the Hounsfield units (HU); one for the hard tissue image with 150 to 300 HU; another for the ST image with -500 to -550 HU. Both soft and hard tissue images were imported into a software, Skull Measure (CyberMed, Seoul, Korea), to measure the distance, between a point on the ST image and a corresponding point on the hard tissue image, which is the ST thickness (Fig. 1).

Measurements

As the site of the ST thickness measurements, 31 landmarks (10 midline and 21 bilateral) were identified according to De Greef et al. (7). Bilateral landmarks were established on one side, the right side of the subject. Table 1 shows the definition of the landmarks used in this study. All descriptions were adopted from the De Greef et al. so a comparison could be made

with their study. Whilst both “perpendicular to skin” and “perpendicular to bone” functions are possible in the program, “perpendicular to bone” was selected in the present study. Four observers carried out the identification of the landmarks; two experienced and another two inexperienced observers. All the landmarks were identified on the ST images and confirmed by the resulting designation on the hard tissue images. One of the experienced observers identified the landmarks twice at a 4 week interval in order to evaluate the intra-observer and inter-observer reproducibility (Table 1).

Statistical analysis

In order to calculate the inter-observer reproducibility, ANOVA and intraclass correlation analysis were used. A Tukey test was performed as a post-hoc comparison to determine the difference in reproducibility between experienced and inexperienced observers. A paired *t*-test was used to calculate the intra-observer reproducibility. The correlation coefficients were calculated using Pearson correlation and reliability coefficient analyses. Statistical data analysis was carried out using SPSS software, version 17.0 for Windows (SPSS Inc, Chicago, IL).

RESULTS

Inter-observer reproducibility

Table 2 illustrates the results of the ANOVA and intraclass correlation analysis including the inter-observer reproducibility of the measurements. Five landmarks (supraglabella, lateral glabella, inferior malar, mental tubercle, and mid-mandibular angle) were identified with statistically significant differences. No statistically significant differences between the observers were found for all remaining landmarks. Intraclass correlation analysis showed that all reliability coefficients were bigger than 0.7 indicating high reproducibility between the

observers (Table 2).

In the post-hoc comparison to determine the differences between the observers, distinct differences were revealed between the experienced (A, B) and inexperienced (C, D) observers. The experienced observers showed a tendency for smaller values than the inexperienced observers. Differences between the two experienced observers (A, B) occurred only at one measurement, the lateral glabella (Table 3).

Intra-observer reproducibility

Table 4 shows the results of a paired *t*-test and correlation analyses showing the intra-observer reproducibility of the measurements. All landmarks were identified without statistically significant differences between the 1st and 2nd measurements indicating high intra-observer reproducibility. Whilst the results of the *t*-test showed high reproducibility for all landmarks, the correlation coefficients showed some variability according to the landmarks, 0.145 to 0.978 for the Pearson correlation and 0.238 to 0.989 for the reliability coefficient. Three landmarks (lower lip, mental eminence, and inferior malar) and two landmarks (mental eminence and inferior malar) showed no statistically significant correlations between the two measurements for the Pearson and reliability analyses respectively (Table 4).

DISCUSSION

Currently facial reconstructions are based on the data sets of the soft tissue thickness obtained from ultrasound analysis. While an ultrasound-based system is an effective tool for measuring soft tissue thicknesses, it has many drawbacks in practical reconstruction. First of all, the measurements are limited. Once the number of measurements has been decided and the measurements are performed, new measurements cannot be added. There are also many

possibilities of measurement error. The thickness is determined according to the transducer orientation and the investigators choose the value of the highest peak, corresponding to the most perpendicular orientation of the transducer to the bone. In addition, precautions must be considered when taking the measurement so as not to indent the facial soft tissues with the ultrasound pen. For this reason, the investigators measure every landmark several times, and choose the largest, corresponding to the minimal soft tissue compression.

However, the use of 3D CT images has greatly reduced the possibility of these errors and provided an opportunity to repeat the measurements. The measurement sites can be added according to the research requirements. Since the hard tissue images are created with an adjustment of HU in addition to the ST images, the landmarks identified on the ST images can be confirmed by the resulting designation on the hard tissue images.

In addition, 3D software enables accurate measurement of ST thickness according to the definition of the measurement. The present study employed specific software named Skull Measure. In this program, both the soft and hard tissue images can be presented simultaneously in a window. Once a landmark is identified on the ST image, the corresponding point is designated automatically on the hard tissue image enabling the investigator to confirm the correct position of the landmark. While the program has both “perpendicular to bone” and “perpendicular to skin” functions, the “perpendicular to bone” function was used for all landmarks in the present study, so that the data would be applicable for forensic facial reconstruction from the skull. Also this would enable comparison with the De Greef et al. (7) study.

While the software calculates the distance between two points using the formula of Euclidean distance automatically, the measurements vary according to the identification of the landmark. The present study aimed to evaluate the reproducibility of ST thickness measurements using 3D CT images. Particular attention was paid to investigate if the

definition of the landmarks described in the previous articles can also be used in the 3D CT images.

The results of ANOVA and intraclass correlation analysis to determine the inter-observer reproducibility showed that majority of landmarks were identified with little differences between the observers. This suggests that the use of CBCT images is validated for the measurement of facial ST thickness. In particular, the results of intraclass correlation analysis showed high values, over 0.7, at all landmarks.

The results of ANOVA showed statistically significant differences between the observers in 5 out of the 31 landmarks; supraglabella, lateral glabella, inferior malar, mental tubercle, and mid-mandibular angle. It is possible that low reproducibility originates from insufficient description of the landmarks for supraglabella and mental tubercle. Both landmarks are described as “most anterior” and this term can be understood differently. It can be determined with the reference to a certain line, such as the true vertical, or simply as “most prominent”. It is suggested that the reproducibility could be increased with the use of a more precise description of the landmarks. Plooiij et al. (12) demonstrated that the redefinition of some soft tissue landmarks resulted in more accurate and reliable 3D soft tissue analysis using 3D stereophotogrammetry.

For the lateral glabella landmark low reproducibility between the observers may be due to the lack of understanding of the anatomical structures. While the definition of the landmark is “junction of the frontal, maxillary, and lacrimal bone”, some observers in the present study failed to recognize the bony structure properly, particularly the lacrimal bone. In addition, the low reproducibility is due partly to the method for calculating the distance in the computer program. While all thicknesses were measured using the “perpendicular to bone” function, the thicknesses can vary even with small differences in the position of the landmark where the bony surface is concave such as at the junction of 3 bony parts. In the area of an irregular

bony surface, the measurement manner of “perpendicular to skin” appears to be more appropriate in terms of reproducibility. The same interpretation applies to measurements at the inferior malar. It was found that resulting hard tissue point was designated frequently on the alveolar area which is more inferior than the definition of the landmark, “just under the zygomatic process”. Some observers repeated the measurement to identify the landmark until the resultant point appeared on the area just under the zygomatic process, whereas other observers assumed that it was sufficient once they had identified the landmark properly on the ST images. This difference resulted in low reproducibility between the observers. It is suggested that measurement “perpendicular to skin” would increase reproducibility as the soft tissue in the area is flat compared to the corresponding bony area. However the use of the “perpendicular to skin” function would make translation of these measurements to the skull for facial reconstruction more difficult, as the tissue depth pegs are attached prior to the reconstruction of the face.

In the case of the mid-mandibular angle point, which showed the lowest reproducibility between observers, it is possible that the description of the landmark, inferior border of the mandible, lined up vertically with the supra M2, is unsuitable for 3D CT images. The landmark cannot be identified properly on the 3D images, whereas the inferior border of the mandible can be palpated when measuring the ST thickness using an ultrasound device. Although the resulting position on the bony surface can be confirmed on the 3D hard tissue images, repeated identification of the landmark is time-consuming, and can be a source of discrepancy between observers. It is suggested that the reproducibility could be increased by identifying the landmark on the hard tissue images, rather than the soft tissue. In addition, the description of the landmark needs to be redefined according to the characteristics of the 3D images in order to increase the reproducibility of the measurement.

In the post-hoc comparison to determine the differences between observers, there were

distinct differences between the experienced and inexperienced observers. This suggests a learning curve exists for identification of the landmarks on 3D images. In other words, the reproducibility can be increased by training and repetition. Differences between two experienced observers occurred only at one measurement, lateral glabella, indicating that the ST thickness measurements can be obtained with high inter-observer reproducibility once the observers have been adequately trained.

The results of the *t*-test to determine the intra-observer reproducibility showed that all landmarks were identified without statistically significant differences between the first and second measurements, indicating high reproducibility. This indicates that the CBCT images can be used reliably to measure the facial ST thickness for the purpose of facial reconstruction.

In correlation analyses, some landmarks, such as lower lip, mental eminence, and inferior malar, showed poor correlations between the two measurements. Considering that the resulting hard tissue point is designated on the upper or lower incisors according to the vertical position of the incisors when identifying the landmark of the lower lip, it is likely that the reproducibility of the measurement might be increased by identifying the landmark on the hard tissue images, rather than the soft tissue.

The low reproducibility of measurements at the mental eminence may be due to the convexity of the bony surface at this area. Since all thicknesses were measured using the “perpendicular to bone” function, a small difference in the position on the bony surface created wide variation in the measurement.

While the ST-based approach is necessary for ultrasound analysis where the skull is not visualised, the ST or hard tissue-based approach can be selected freely on the 3D images according to the characteristics of the landmarks to increase the reproducibility. Previous studies (13,14) examined both the hard and soft tissue landmarks in the 3D images, and

reported that the hard tissue points were easier to localize than soft tissue landmarks. This suggests that a soft tissue-based description of the considerable number of landmarks needs to be changed to a hard tissue-based definition in the CBCT images to increase the reproducibility.

In summary, the facial soft tissue thickness measurements on the CBCT images showed high inter- and intra-observer reproducibility. The results of the present study suggest that the CBCT images can be used reliably for the purpose of facial reconstruction. While some landmarks showed low reproducibility, the reliability may be increased by redefining the landmarks according to the characteristics of the 3D images.

REFERENCES

1. Snow CC, Gatliff BP, McWilliams KR. Reconstruction of facial features from the skull: an evaluation of its usefulness in forensic anthropology. *Am J Phys Anthropol* 1970;33(2):221-8.
2. Wilkinson C. *Forensic Facial Reconstruction*. Cambridge: Cambridge University Press, 2004.
3. De Greef S, Willems G. Three-dimensional cranio-facial reconstruction in forensic identification: latest progress and new tendencies in the 21st century. *J Forensic Sci* 2005;50(1):12-7.
4. Manhein MH, Listi GA, Barsley RE, Musselman R, Barrow NE, Ubelaker DH. In vivo facial tissue depth measurements for children and adults. *J Forensic Sci* 2000;45(1):48-60.
5. El-Mehallawi IH, Soliman EM. Ultrasonic assessment of facial soft tissue thicknesses in adult Egyptians. *Forensic Sci Int* 2001;117(1-2):99-107.
6. Wilkinson CM. In vivo facial tissue depth measurements for white British children. *J Forensic Sci* 2002;47(3):459-65.
7. De Greef S, Claes P, Vandermeulen D, Mollemans W, Suetens P, Willems G. Large-scale in-vivo Caucasian facial soft tissue thickness database for craniofacial reconstruction. *Forensic Sci Int* 2006;159 Suppl 1:26-46.
8. Phillips VM, Smuts NA. Facial reconstruction: utilization of computerized tomography to

measure facial tissue thickness in a mixed racial population. *Forensic Sci Int* 1996;83(1):51-9.

9. Mah JK, Danforth RA, Bumann A, Hatcher D. Radiation absorbed in maxillofacial imaging with a new dental computed tomography device. *Oral Surg Oral Med Oral Pathol Oral Radiol Endod* 2003;96(4):508-13.

10. Tsiklakis K, Donta C, Gavala S, Karayianni K, Kamenopoulou V, Hourdakakis CJ. Dose reduction in maxillofacial imaging using low dose Cone Beam CT. *Eur J Radiol* 2005;56(3):413-7.

11. Swennen GR, Schutyser F. Three-dimensional cephalometry: spiral multi-slice vs cone-beam computed tomography. *Am J Orthod Dentofacial Orthop* 2006;130(3):410-6.

12. Plooij JM, Swennen GR, Rangel FA, Maal TJ, Schutyser FA, Bronkhorst EM, Kuijpers-Jagtman AM, Bergé SJ. Evaluation of reproducibility and reliability of 3D soft tissue analysis using 3D stereophotogrammetry. *Int J Oral Maxillofac Surg* 2009;38(3):267-73.

13. Farkas LG. *Anthropometry of the Head and Face*. New York: Raven Press, 1994.

14. Cavalcanti MG, Rocha SS, Vannier MW. Craniofacial measurements based on 3D-CT volume rendering: implications for clinical applications. *Dentomaxillofac Radiol* 2004;33(3):170-6.

Table 1. Description of the anatomical landmarks utilized for tissue depth measurement

Landmarks	Description†
Midline landmarks	
Supraglabella	Most anterior point on midline
Glabella	Crosspoint between midline and supraorbital line
Nasion	Midpoint of the fronto-nasal suture
End of nasal	Junction between bone and cartilage of the nose
Mid-philtrum	Centred between nose and mouth on midline
Upper lip	Midline on the upper lip
Lower lip	Midline on the lower lip
Chin-lip fold	Midline centred in fold chin, below lips
Mental eminence	Centred on most anteriorly projecting point of chin
Beneath chin	The vertical measure of the soft tissue on the most inferior point of the chin
Unilateral landmarks	
Frontal eminence	Centred on pupil, most anterior point of the forehead
Supraorbital	Centred on pupil, just above eyebrow
Lateral glabella	Junction of the frontal, maxillary, and lacrimal bones on the medial bone of the orbit
Lateral nasal	Side of the bridge of the nose on the Frankfurt Horizontal plane
Suborbital	Centred on pupil, just under infra-orbital margin

Inferior malar	Centred on pupil, just interior to zygomatic process
Lateral nostril	Next to the most lateral point of the alar border
Naso-labial ridge	The prominence either side of the philtrum
Supra canina	Vertically lined up with the cheilion, on the horizontal level of the Mid-philtrum
Sub canina	Vertically lined up with the cheilion, on the horizontal level of the Chin-lip fold
Mental tubercle anterior	Most prominent point on the lateral bulge of the chin mound
Mid lateral orbit	Vertically centred on the orbit, next to the lateral orbital border
Supraglenoid	Root of the zygomatic arch just anterior to the ear
Zygomatic arch	Most lateral curvature of the zygomatic bone
Lateral orbit	Lined up with the lateral border of the eye on the centre of the zygomatic process
Supra M2	Cheek region, lateral: lined up with nasal base; vertical: lined up beneath lateral border of the eye
Mid masseter	Middle of the masseter, the halfway point between the supraglenoid and the gonion
Occlusal line	Border of the masseter, on vertical level of the cheilion
Sub M2	Below the second molar on horizontally lined up with Supra M2
Gonion	At the angle of the mandible
Mid mandibular	Inferior border of the mandible, vertically lined up with Supra M2

† The present study used same description as that in De Greef et al's study (2006).

Table 2. Results of the ANOVA and intraclass correlation analysis showing the inter-examiner reproducibility of the soft tissue depth measurements (n=20) using cone-beam CT images

<i>Measurements</i>	<i>A</i>	<i>B</i>	<i>C</i>	<i>D</i>	<i>ANOVA</i>	<i>ICC</i>
	<i>Mean±SD</i>	<i>Mean±SD</i>	<i>Mean±SD</i>	<i>Mean±SD</i>	<i>(P value)</i>	
Midline landmarks (mm)						
Supraglabella	5.4±1.0	4.7±0.9	5.4±0.8	5.5±0.9	0.027*	0.878
Glabella	5.7±0.7	5.7±0.8	5.7±0.8	5.9±0.7	NS	0.891
Nasion	6.3±1.0	6.5±1.0	6.4±0.8	6.8±1.0	NS	0.957
End of nasal	2.6±1.2	2.7±1.1	2.7±1.2	2.9±1.0	NS	0.960
Mid-philtrum	11.6±1.5	11.9±1.7	11.8±1.7	11.9±1.5	NS	0.913
Upper lip	11.2±1.7	11.4±1.9	11.7±1.7	12.0±1.8	NS	0.963
Lower lip	12.0±1.9	13.1±1.6	12.5±1.3	12.4±1.4	NS	0.804
Chin-lip fold	10.9±1.1	11.3±1.3	11.0±1.2	10.9±1.3	NS	0.833
Mental eminence	12.1±1.4	11.4±1.5	11.8±1.6	12.1±1.6	NS	0.919
Beneath chin	7.6±1.6	7.3±1.7	7.0±1.4	7.5±1.7	NS	0.894
Bilateral landmarks (mm)						
Frontal eminence	5.8±1.2	4.9±1.0	5.2±1.3	5.8±1.4	NS	0.934
Supraorbital	6.9±1.5	7.2±0.9	6.7±1.1	7.0±1.3	NS	0.887

Lateral glabella	8.5±2.0	6.8±1.6	7.5±1.6	7.8±1.9	0.033*	0.865
Lateral nasal	6.7±1.6	5.9±1.1	6.3±1.4	6.3±1.8	NS	0.704
Suborbital	7.4±1.2	7.4±1.2	7.3±1.3	7.7±1.4	NS	0.932
Inferior malar	17.0±2.6	15.7±2.2	17.8±2.4	17.6±2.5	0.034*	0.729
Lateral nostril	13.5±1.6	13.1±1.9	13.1±3.4	13.9±2.1	NS	0.762
Naso-labial ridge	12.0±1.5	12.1±1.6	12.6±1.8	12.7±1.5	NS	0.773
Supra canina	10.8±1.5	11.2±2.1	10.7±1.2	11.3±1.2	NS	0.725
Sub canina	11.9±1.7	12.7±1.6	12.6±1.6	12.5±1.5	NS	0.878
Mental tubercle anterior	10.0±1.7	9.6±2.0	10.3±1.5	11.2±1.8	0.045*	0.914
Mid lateral orbit	5.4±1.1	5.6±1.0	5.2±1.4	5.9±1.4	NS	0.900
Supraglenoid	12.6±2.1	12.6±1.8	12.6±2.4	12.8±2.2	NS	0.855
Zygomatic arch	8.7±1.6	8.5±1.5	8.5±1.7	9.3±1.8	NS	0.969
Lateral orbit	9.9±1.5	9.8±1.5	9.6±1.6	10.0±1.8	NS	0.946
Supra M2	28.1±3.1	27.8±2.7	28.0±3.0	28.7±3.5	NS	0.820
Mid masseter	18.3±3.0	17.8±2.5	17.5±3.0	17.9±2.4	NS	0.947
Occlusal line	21.8±2.5	22.6±2.4	22.4±2.4	22.4±2.1	NS	0.976
Sub M2	21.1±2.9	19.9±2.4	20.3±2.9	20.8±2.7	NS	0.907
Gonion	13.6±2.5	12.5±3.4	12.6±2.9	12.8±2.9	NS	0.942
Mid mandibular	7.9±1.5	8.4±1.7	9.8±2.6	9.8±1.8	0.002**	0.831

NS, Not significant; ICC, Intraclass correlation analysis; Excellent>0.800. * $p < 0.05$; ** $p < 0.01$.

Table 3. Post-hoc comparison by Tukey grouping for the soft tissue depth measurements between examiners using cone-beam CT images

<i>Measurements</i>	<i>Mean±SD</i>				<i>Significance</i>
Midline landmarks (mm)					
Supraglabella	B	A	C	D	
	4.7±0.9	5.4±1.0	5.4±0.8	5.5±0.9	0.027
Bilateral landmarks (mm)					
Lateral glabella	B	C	D	A	
	6.8±1.6	7.5±1.6	7.8±1.9	8.5±2.0	0.033
Inferior malar	B	A	D	C	
	15.7±2.2	17.0±2.6	17.6±2.5	17.8±2.4	0.034
Mental tubercle anterior	B	A	C	D	

	9.6±2.0	10.0±1.7	10.3±1.5	11.2±1.8	0.045
Mid mandibular	A	B	D	C	
	7.9±1.5	8.4±1.7	9.8±1.8	9.8±2.6	0.002

Groups connected by horizontal bars were not significantly different ($p < 0.05$).

Table 4. Results of the *t*-test and correlation analyses showing the intra-examiner reproducibility of soft tissue depth measurements (n=20) using cone-beam CT images

<i>Measurements</i>	<i>1st</i>	<i>2nd</i>	<i>Significance</i>	<i>Pearson correlation</i>	<i>Reliability</i>
	<i>measure</i>	<i>measure</i>		<i>coefficient</i>	<i>coefficient</i>
	<i>Mean±SD</i>	<i>Mean±SD</i>			
Midline landmarks (mm)					
Supraglabella	5.4±1.0	5.4±1.0	NS	0.968***	0.983***
Glabella	5.7±0.7	5.7±0.7	NS	0.978***	0.989***
Nasion	6.3±1.0	6.4±1.1	NS	0.937***	0.960***
End of nasal	2.6±1.2	2.8±1.1	NS	0.934***	0.966***
Mid-philtrum	11.6±1.5	11.6±1.7	NS	0.973***	0.983***
Upper lip	11.2±1.7	11.1±1.5	NS	0.866***	0.925***
Lower lip	12.0±1.9	12.9±1.5	NS	0.389	0.549*
Chin-lip fold	10.9±1.1	11.2±1.2	NS	0.731***	0.844***
Mental eminence	12.1±1.4	12.5±1.4	NS	0.170	0.290
Beneath chin	7.6±1.6	7.0±1.2	NS	0.697**	0.797**
Bilateral landmarks (mm)					
Frontal eminence	5.8±1.2	6.6±1.3	NS	0.739***	0.850***
Supraorbital	6.9±1.5	7.2±1.0	NS	0.525	0.656*
Lateral glabella	8.5±2.0	8.6±1.9	NS	0.655**	0.791*

Lateral nasal	6.7±1.6	6.6±1.2	NS	0.724***	0.817***
Suborbital	7.4±1.2	7.1±1.5	NS	0.730***	0.838***
Inferior malar	17.0±2.6	18.1±1.8	NS	0.145	0.238
Lateral nostril	13.5±1.6	13.6±1.8	NS	0.712***	0.827***
Naso-labial ridge	12.0±1.5	11.9±1.5	NS	0.938***	0.968***
Supra canina	10.8±1.5	10.5±1.2	NS	0.801***	0.871***
Sub canina	11.9±1.7	12.1±1.0	NS	0.513*	0.622*
Mental tubercle anterior	10.0±1.7	9.3±1.8	NS	0.828***	0.905***
Mid lateral orbit	5.4±1.1	5.3±1.0	NS	0.894***	0.941***
Supraglenoid	12.6±2.1	12.4±1.6	NS	0.824***	0.887***
Zygomatic arch	8.7±1.6	8.4±1.5	NS	0.937***	0.967***
Lateral orbit	9.9±1.5	9.6±1.5	NS	0.932***	0.965***
Supra M2	28.1±3.1	27.9±2.5	NS	0.660**	0.784**
Mid masseter	18.3±3.0	18.5±2.7	NS	0.936***	0.963***
Occlusal line	21.8±2.5	22.2±2.5	NS	0.955***	0.977***
Sub M2	21.1±2.9	22.5±2.9	NS	0.642**	0.782**
Gonion	13.6±2.5	12.8±2.8	NS	0.616**	0.759**
Mid mandibular	7.9±1.5	7.2±1.2	NS	0.616**	0.756**

NS, Not significant; * $p < 0.05$; ** $p < 0.01$; *** $p < 0.001$.

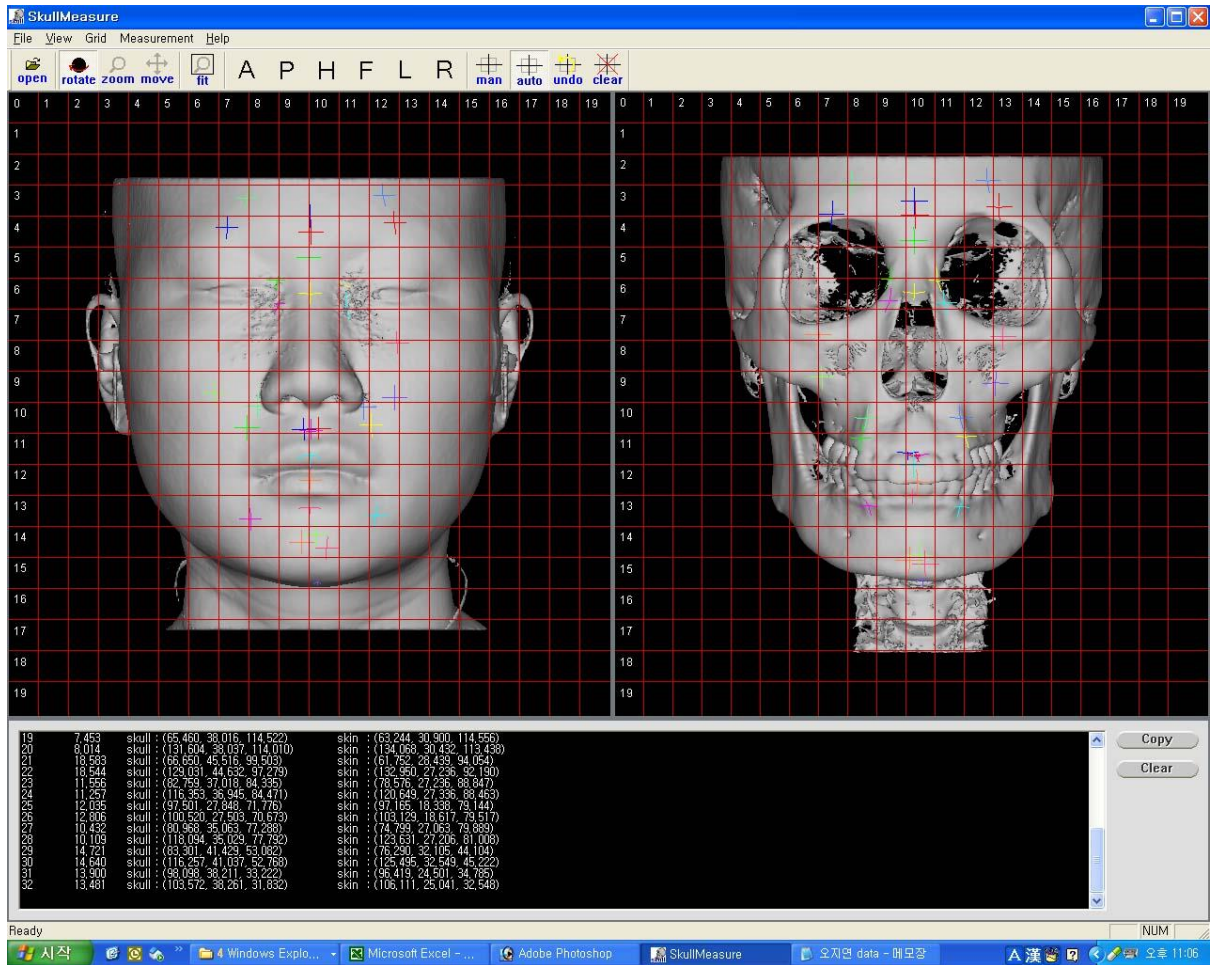


Fig 1. A window of the Skull Measure program used to measure soft tissue depths on cone-beam CT images. Both soft and hard tissue images are rotated freely so the landmarks are identified accurately according to their definitions. Once the position is established on the soft tissue image, enabling the corresponding point is designated automatically on the hard tissue image enabling the investigator to confirm the correct position of the landmark.